A 3-D finite element analysis of the sunflower (*Helianthus annuus* L.) fruit. Biomechanical approach for the improvement of its hullability

L.F. Hernández [a,c,*], P.M. Bellés [b,c]

[a] *Laboratorio de Morfología Vegetal, Depto de Agronomía, Universidad Nacional del Sur, 8000 Bahía Blanca, Argentina*
[b] *Depto de Ingeniería – IMA, Universidad Nacional del Sur, 8000 Bahía Blanca, Argentina*
[c] *Comisión de Investigaciones Científicas (CIC-PBA), 1900 La Plata, Argentina*

Abstract

For the sunflower fruits, hullability (**H**) is a technical parameter that defines how easily the hull can be broken and set apart from the kernel. **H** mainly depends on the morphology of the fruit and the biochemical properties of the hull. Finite element analysis (FEA) was used to model the mechanical behavior of the sunflower fruit hull after the fruit impact. A 3-D model of an entire fruit was designed in terms of strain incompatibilities between two different tissues, parenchyma and sclerenchyma. Impact was simulated for three orientations of the fruit: longitudinal, transversal and lateral; and for two thicknesses of the hull: 100 μm and 300 μm. The validation of the FEA model was made based on a comparison of theoretical calculations and experimental data. It was noticed that the points of contact between the above mentioned tissues – with different mechanical properties – and the longitudinal parenchymatous rays of the hull were the main structural sites prone to fail mechanically after impact.

The simulated patterns of failure closely agree with those observed after subjecting fruits to compressive loading. The procedure described in this work could be useful to quantify and qualify, under different hull structural parameters, the distribution and magnitude of stresses generated in the hull during industrial mechanical hulling. It can be considered the first step of a protocol of analysis leading to a genetic improvement of **H**.
© 2005 Elsevier Ltd. All rights reserved.

Keywords: Finite element analysis; Hullability; Hull; Impact analysis; Mechanical and fracture properties; Modeling; Pericarp; Sunflower

1. Introduction

Sunflower grains are botanically defined as fruits. They are composed by a thin outer shell, the pericarp, also known as "hull", that surrounds and contains the seed, usually named "kernel". The seed contains the largest proportion of oil that is found in a fruit (Seiler, 1997).

Sunflower fruits are hulled before they enter in the industrial process of oil extraction. Hulling consists in the separation of the pericarp from the seed. The hulling machinery used in the oil industry frequently is based on the principle of impact. Large propellers centrifugally throw the fruits at high speed (15–30 m s^{-1}) against a hard surface where their pericarps totally or partially break apart.

The pericarp accounts for 20–26% (dry basis) of the total fruit weight and is a brittle structure composed by different tissues which have different physical and biochemical properties. The two main ones found in a mature fruit are parenchyma and sclerenchyma (Esau, 1977). The later one has a high proportion of lignin (20–25% db; Seiler, 1997). These tissues are transversally and longitudinally arranged forming compact bundles defined as rays (Lindström, Pellegrini, & Hernández, 2000; Seiler, 1997).

---
* Corresponding author. Address: Laboratorio de Morfología Vegetal, Depto de Agronomía, Universidad Nacional del Sur, 8000 Bahía Blanca, Argentina. Tel.: +54 0291 4566131; fax: +54 0291 4595127.
E-mail address: lhernan@criba.edu.ar (L.F. Hernández).

The ability of the pericarp to break and to separate from the seed can be quantitatively defined with an index named hullability (**H**) (Denis, Coelho, & Vear, 1994; Denis, Dominguez, & Vear, 1994). It is calculated as (MHW/THW) × 100, where: MHW = weight of the pericarp obtained using small laboratory hulling machines that simulate the industrial process and THW = total weight of the pericarp obtained by manual hulling.

The orientation of the fruit inside the hulling machine during the impact can affect the magnitude of the pericarp breakage during the process. **H** is higher if the fruit impacts longitudinally or transversally than if it impacts radially, on its convex sides (Leprince-Bernard, 1990). Moreover hullability is closely related to morphological, histological and biomechanical properties of the pericarp. Its magnitude mainly relies on various pericarp structural properties such as its thickness (Dedio, 1993; Dedio & Dorrell, 1998; Denis & Vear, 1996) and number of parenchymatic rays, cell lignification and moisture content (Beauguillaume & Cadeac, 1992; Gupta & Das, 2000; Leprince-Bernard, 1990).

Fruit and seed size (Morrison, Akin, & Robertson, 1981; Beauguillaume & Cadeac, 1992; Leprince-Bernard, 1990; Lindström et al., 2000; Tranchino, Melle, & Sodini, 1984) and oil content (Baldini & Vannozzi, 1996; Denis et al., 1994; Denis & Vear, 1996; Fick & Miller, 1997) play also a very important role in the magnitude of **H**.

Some of these properties could be genetically modified (Fick & Miller, 1997) or changed with environmental growth conditions (Dorrell & Vick, 1997) and crop management (Baldini & Vannozzi, 1996; Dedio & Dorrell, 1998).

Using biotechnological techniques it is now also possible to genetically transform the mechanical properties of plant tissues, particularly modifying the metabolism for lignin synthesis (Boudet, Kajita, Grima-Pettenati, & Goffner, 2003; Hepworth & Vincent, 1998; Pilate, Guiney, & Halpin, 2002; Ralph, MacKay, & Hatfiled, 1997; Whetten, Mackay, & Sederoff, 1998).

For improving **H** by using these novel technologies the optimisation of the histological architecture of the pericarp should be considered. The accurate definition of its constitutive tissues, how they are distributed in fruits with different **H** and its biomechanical properties are then important variables to be defined. In this particular case a more precise approach should be taken in order to specify, for each biostructural component, the best distribution and quality of tissues.

Predicting the localization of the yielding sites and quantifying the magnitude of stresses produced when the fruit impacts during mechanical hulling, may help to define the best tissue distribution and composition that conforms an optimised pericarp histological architecture.

If the stresses and deformation of the hull can be predicted, the interpretation of the results requires a knowledge of the relationships among stresses, strains, and failure i.e. cracking or splitting of the fruit caused by cell wall rupturing or tissue separation. This information then could allow us to efficiently use the available biotechnological tools to improve **H**.

Several theories of failure for plant tissue have been proposed (Niklas, 1992). Generally is assumed that plant tissue may fail when normal strain reaches a critical value. In this work the biomechanical identification of yielding sites in the pericarp were estimated using a numerical approach, validating the results with laboratory mechanical tests.

2. Materials and methods

2.1. Anatomy of the pericarp

The anatomy of the pericarp was studied in two sunflower genotypes with highly contrasting morphology, i.e. small fruits with thin pericarp (genotype Morgan MG2) and larger fruits with thick pericarp (genotype Morgan M734) from transverse, longitudinal and tangential sections of whole fruits. Sections were appropriately stained (Ruzin, 1999) to obtain a detailed location of the main tissues within the pericarp and to determine their distribution according to their lignification level. This information was used to elaborate a model of tissue distribution.

2.2. Biomechanical properties of the tissues

The modulus of elasticity of the main tissues (parenchyma [R_p] and sclerenchyma [T_e] rays; Niklas, 1992; Wainwright, Biggs, Currey, & Gosline, 1982), were calculated from tensile and compressive tests made on longitudinal pericarp's segments of known dimensions. We use a micromechanical testing device for small plant samples designed in our laboratory. It was based in a high precision electronic balance (AND ER-180A, A&D Co. Ltd., Japan), mounted on a cantilever system holding an automated small displacement screw driven by an actuator. Samples of 10.0–12.0 mm length and 2.0 mm width and thicknesses of 100 μm for genotype MG2 and 300 μm for genotype M734 were prepared from longitudinal pericarp segments of 25 fruits for each genotype. Samples were gripped in simple-side acting grips and pressed or pulled in three directions (longitudinally [L], radially [R] or transversally [T]) at 5 mm min^{-1}. Relative humidity of all samples was kept at 11% (db). Real time data were collected and downloaded to a PC. From the force–deformation relationships obtained, the transformed stress/strain relationships were used to calculate the elastic moduli of the main tissues (parenchyma and sclerenchyma) for each fruit's orientation (E_L, E_R and E_T).

Poisson ratios for each tissue component and orientation was estimated from data described in the literature (Niklas, 1992; Preston, 1974; Wainwright et al., 1982). Tissue density was determined from the weight of pericarp segments of known dimensions.

Structural elastic modulus (E_{st}; Rowe & Speck, 2000) and the rupture modulus (RM; Niklas, 1992) for the whole fruits of the two genotypes in three orientations was

calculated using uniaxial compression tests with an Instron 1122 universal testing machine (UTM) with a 0–100 kg load cell and an integrator, at a cell's speed of 1.0 mm min^{-1}. The load magnitudes necessary to reach the hull's bioyield point (Gupta & Das, 2000) and to empirically define the breakage pattern were obtained.

2.3. Theoretical approach to the study of the pericarp breakage. Modeling and stress simulation

A three-dimensional finite element model (FEM) of the sunflower fruit pericarp was developed. The finite element method (Logan, 2001) is a numerical procedure especially suited for solving the partial differential equations which describe stresses and strains in biological materials. This method can be used for both static and dynamic structural analyses and allows modeling of irregularly shaped objects which have heterogeneous properties and are subjected to mixed boundary conditions. The equivalent stress analysis is also valid in the case of the modified Von Mises criteria (Logan, 2001).

A 3-D model of the hull was built based on the external shape of randomly selected fruits of the studied genotypes. They were digitised on two orthogonal planes, perpendicular to the longitudinal axis. Using adequate CAD software, contour coordinates of these profiles were obtained and integrated.

The 3-D model was properly meshed (Fig. 1A and B) using the shell structural element (Logan, 2001). The shell-based surface is justified since the whole pericarp is very thin compared with the in-plane dimensions. Three-nodal triangles and 4-nodal squares were used, giving the model a configuration of 2131 elements with 2080 nodes (Logan, 2001).

For the model definition and simplification purposes the hull was considered to be mainly composed by two stabilizing tissues that were incorporated as two independent element groups, the sclerified tissue (T_e) which is heavily lignified and the parenchymatic rays (R_p, Fig. 1B). Another three element groups were defined in order to give the model more realistic structural properties. They where the fruit ends, basal (be) and apical (ae), and the pericarp dorsal border (db) (Fig. 1A).

The seed kernel inside the hull was not included. From empirical experience we hypothesize at this stage that the kernel provided little, if any, resistance to the compression of the hull.

Even though the sunflower hull is made of a composite material like wood (Thibaut, Gril, & Fournier, 2001) with fibres running parallel to the major axis and to the contours of the seed, in this model, the material was modelled as an isotropic material, instead of as a composite.

2.4. Calculation and localization of stresses in the model under simulated impact

The analysis was made using the ACCUPACK/VE routine from ALGOR (vers. 14, Algor Inc., Pittsburgh, PA), a software processor for non-linear calculation to conduct a mechanical event simulation (MES). Impact simulation at
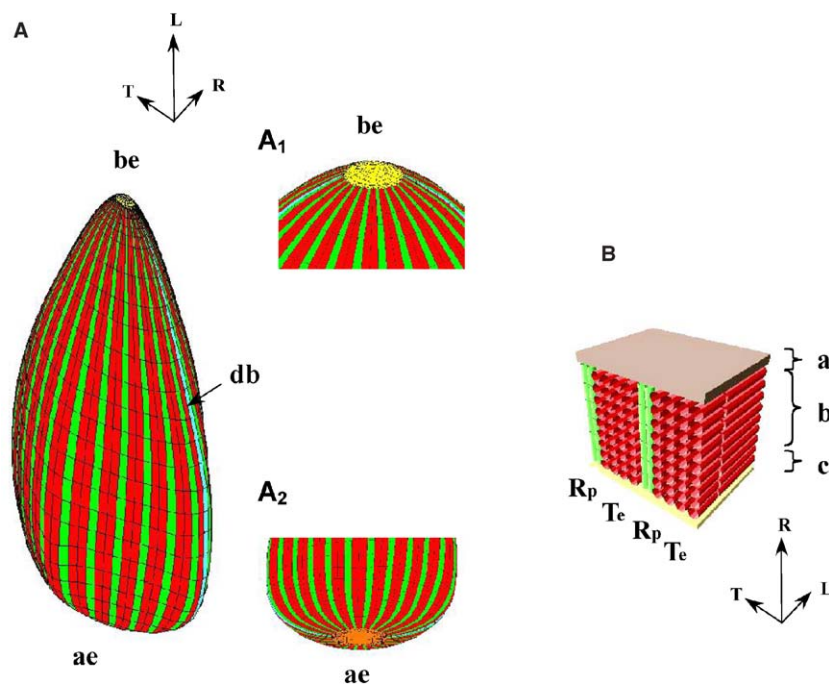

Fig. 1. A: Meshed model of a sunflower fruit in an orthogonal isometric view, after integration of the coordinates in different planes of images taken from full-grown fruits. A_1 and A_2: Details of the basal end (be) and apical end (ae) respectively; db: pericarp's dorsal border. B: Model of the histological components of the pericarp. R_p: ray of parenchyma; T_e: ray of sclerenchyma. Strata a–c are the external epidermis, inner tissue ($R_p + T_e$) and internal epidermis respectively (see also Fig. 2). Coordinate axis in each figure indicates the orientation of the model: *L*–longitudinal, *R*–radial; *T*–transversal.

a speed of 30 m s^{-1} was registered at a capture rate of 100 steps per second.

The magnitudes of tensions and stresses at the site of the fruit's simulated impact against a rigid surface with different orientations were identified, validating the calculated results with those obtained with mechanical tests performed in the laboratory.

2.5. Statistical analysis

The model was loaded to simulate three orientations of impact and combinations of R_p and T_e thicknesses and R_p interdistance. To determine the sensitivity of the input parameters in the model outputs a factorial analysis was made using the Taguchi's robust parameter design (Dar, Meakin, & Aspden, 2002). The magnitudes of stress (MN) obtained after several runs of the model were transformed as $MN_T = -10\log_{10}(MN^2)$ and compared. The statistical analysis was performed with SAS statistical software (JMP statistical software version 4.0.4; SAS Inc., Cary, NC).

3. Results and discussion

The pericarp of the sunflower fruit shows an orderly arrangement of tissues distributed in layers. From the outside there is an epidermis of rectangular cells (Fig. 2) protected by a cuticle; the hypodermis, composed of cells with thin walls and an amorphous layer of phytomelanin (Fig. 2); a layer of numerous rows of elongated polygonal sclerenchymatic cells, which strengthens the structure towards the longitudinal axis of the fruit and with a stiffness gradient of radial direction that increases from the outside to the inside of the fruit (T_e; Fig. 2A and B). This layer is interrupted at regular intervals (separated by 100–300 μm) by parenchymatic rays (R_p; Fig. 2A and B), numerous parenchymatic cells with thin walls loosely arranged and an inner epidermis (Fig. 2A and B). This anatomical description agrees with that documented by Lindström et al. (2000) in fruits of several modern sunflower genotypes.

The strain/stress relationships calculated from the average load–deformation curves obtained in the laboratory tests for different fruit morphology and orientations are presented in Fig. 3. Maximum magnitudes for each test differ significantly between genotypes and orientations. For MG2 (Fig. 3A), the three maximum magnitudes at the bioyield point were 2–4 times smaller than for the M734 genotype (Fig. 3B). From the laboratory load tests for different fruit morphology and orientations (Fig. 4), the breakage pattern show lines of fracture in the pericarp oriented in a parallel direction towards the major axis of the fruit (Fig. 4A–C).
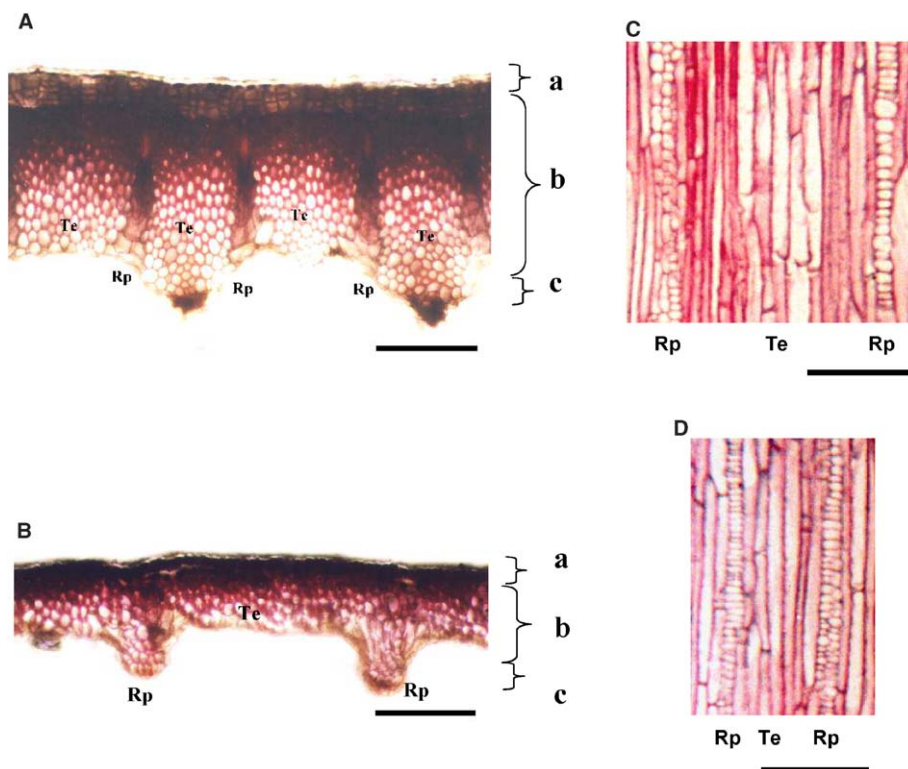

Fig. 2. Histology of the pericarp. Portion of a transversal cut showing the distribution of tissues for the genotypes M734 (A) and MG2 (B); a: epidermis + hipodermis; b: sclerified cells; c: compressed inner parenchyma cells. Correspondent tangential longitudinal portion of the pericarp for the genotypes M734 (C) and MG2 (D) where the distribution and separation of the parenchyma rays (R_p) and the sclerified tissue (T_e) are observed. Bar = 100 μm.
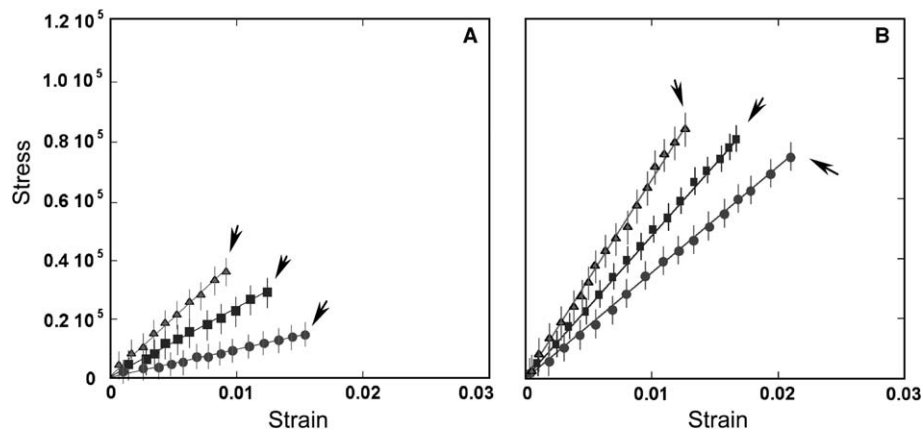
Fig. 3. Strain–stress relationship calculated from force–deformation data obtained from tissue segments of full-grown fruits of the genotypes MG2 (A) and M734 (B), when tested longitudinally (▲), transversally (■) or radially (●). A. Genotype MG2. Pericarp's thickness = 100 μm; average R_p separation = 300 μm. B. Genotype M734. Pericap's thickness = 300 μm; average R_p separation = 100 μm. Each point is the average value of 25 determinations. Arrows indicate the bioyield point.
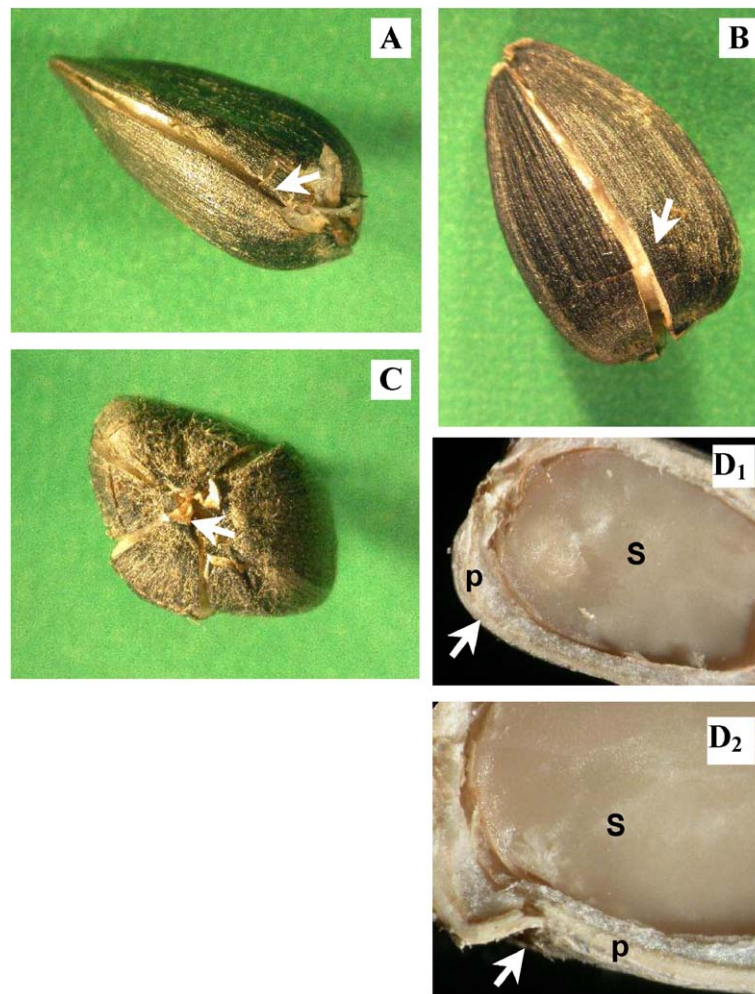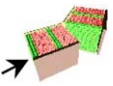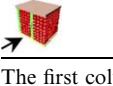

Fig. 4. Hull's breakage pattern at the bioyield point for different fruit's orientations at the moment of impact: A, longitudinally, B, radially or C, transversally. Arrows indicate the site of impact. D: inner view from a longitudinal cut of a whole fruit of genotype M734, showing the relative position of the seed (s) inside the pericarp (p) before (D_1) and at the moment (D_2) of impact for transversally oriented fruits. Note that the pericarp has already failed (D_2; arrow) and the forces generated during the impact have not yet been transduced to the seed.

Mechanical properties of the histological components in the model of Fig. 1B, for three impact orientations are described in Table 1. In the sclerified tissue Young's modulus for the longitudinal direction is four times higher than that in the tangential direction (Fig. 4B and C; Table 1).

A graphical representation from the numeric simulation for three impact orientations using the model of Fig. 1 is shown in Fig. 5. The analysis was conducted using three different values of the moduli of elasticity as indicated in Table 1. The magnitudes of the stresses generated at the site of impact are shown in Table 2. The highest values were observed in the area of impact (Fig. 5A–C), indicating that immediately after the impact the structure could sustain an irreversible damage leading to its instability and rupture. Stresses are propagated basipetally and radiated (Fig. 5D–F) mainly as a consequence of the alternance of rays with quite different mechanical properties (Table 1) and of its longitudinal distribution in the pericarp matrix (Fig. 1A and B).

Table 1
Mechanical properties of the histological components used in the FE model of Fig. 1 for three impact orientations

Model orientation at the time of impact	Morphological and mechanical properties of the main model's components						
	Thickness (μm)		Mechanical parameters		Apical end	Basal end	Dorsal border
	T_e	R_p	T_e	R_p			
			E: 57.0	E: 30.0	E: 30.0	E: 30.0	E: 10.0
	100	100	δ: 800	δ: 300	δ: 600	δ: 700	δ: 600
	300	300	v: 0.25	v: 0.45	v: 0.40	v: 0.25	v: 0.25
			E: 70.0	E: 40.0	thick: 300	thick: 350	thick: 300
	100	100	δ: 800	δ: 300			
	300	300	v: 0.25	v: 0.45			
			E: 230.0	E: 40.0			
	100	100	δ: 800	δ: 300			
	300	300	v: 0.25	v: 0.45			

The first column describes the orientation of the model for impact.
R_p: ray of parenchyma; T_e: ray of sclerenchyma; E: elastic modulus (MN m^{-2}); δ: density (kg m^{-3}); v: Poisson coefficient; thick: tissue thickness (μm).
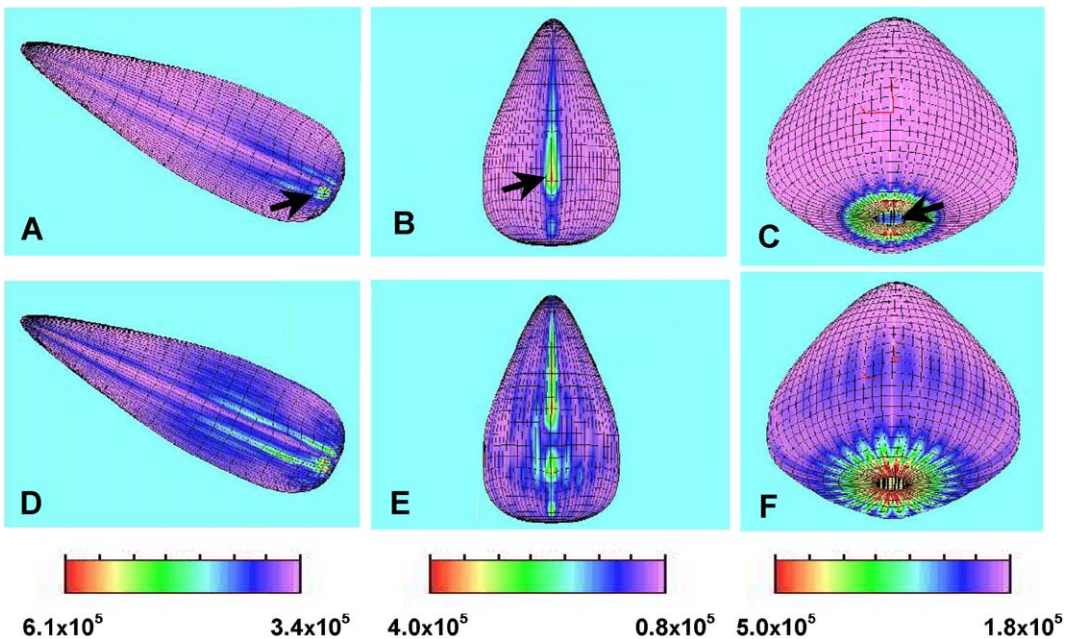

Fig. 5. Stress distribution during impact at a speed of 30 m s^{-1} obtained from the FE analysis. Stress magnitudes are shown for three orientations: transversal (A, D), radial (B, E) and longitudinal (C, F), and, in a sequence from the beginning of the impact (t_0; A–C) and after a 0.03 s (D–F). The stress pattern is distributed following the alternate arrangement of the tissues that conform the model, from the site of impact (arrow in A–C). This pattern resembles the pericarp breakage pattern observed in real fruits (Fig. 4, A–C respectively). Color scale bar indicates gradient areas (from maximum to minimum) of VonMises stress (N m^{-2}) in the simulation.

Table 2
Calculated and simulated tensions at three orientations of impact

Fruit orientation	Tissue thickness (μm)		E_{st}[a]	CFT[b]	VM[c]
	T_e	R_p	Calculated (Lab. test) (N m^{-2})	Theoretical fracture stress (Lab. test) (N m^{-2})	Obtained in the simulation (N m^{-2})
	100	100	9.11×10^6	0.84×10^5	0.88×10^5
	300	300	35.10×10^6	3.22×10^5	4.02×10^5
	100	100	22.33×10^6	2.05×10^5	1.83×10^5
	300	300	48.27×10^6	4.44×10^5	5.20×10^5
	100	100	37.48×10^6	3.44×10^5	3.51×10^5
	300	300	66.25×10^6	6.09×10^5	5.89×10^5

R_p: Ray of parenchyma; T_e: Ray of schlerenquima; RM: Rupture modulus.
[a] E_{st}: structural elastic modulus, calculated for the whole fruit from laboratory tests and 7% relative humidity (dwb).
[b] CFT: critical fracture tension (N m^{-2}) estimated as E_{st}. 0.0092 (from Niklas, 1992).
[c] VM: VonMises obtained from the FE model after MES. These values were captured at the moment of the simulated impact from two pericarp thicknesses: $R_p = 100$, 300 μm and $T_e = 100$, 300 μm.

The comparison between the stress magnitudes, particularly the rupture modulus (Niklas, 1992), obtained from laboratory tests and those calculated from the FE model (Table 2) show that the regions of the hull able to collapse are longitudinally distributed, parallel to the parenchymatic rays. The stress patterns calculated in the simulation (Fig. 5) agree with the breakage pattern observed in laboratory tests (Fig. 4). The alternate distribution or R_p and T_e (Fig. 2), is the main reason to give the model its structural response.

The fruit model presented here is based only in the hull, assuming that a very soft seed, that usually does not fill its interior (Fig. 4D), will not interfere in the stress patterns developed immediately after impact. Fig. 4D shows longitudinal cross-sectional views of a mature fruit before and after a transversal impact. Clearance produced by spongy tissue (the inner pericarp, depicted in Fig. 2A and B) between the hull and kernel is conspicuous along the entire inner surface of the hull (Fig. 4D).

In Fig. 4D it is also shown that after impact the structure of the seed it is not compromised. It was easily observed in the fruits of the genotype M734 but can be generally defined for every fruit if the seed fills completely or partially the inner cavity of the pericarp. In any case there is an intermediate spongy tissue, soft and elastic, that will be able to absorb the energy generated from the outer site of impact to the inner components of the fruit (Fig. 4D).

The statistical analysis made to better qualify the effects that different structural parameters and orientations had on the output of the simulation are presented in Fig. 6. A full factorial analysis was selected as the approach because all permutations of the test conditions had been conducted and the data were available for this study. In this study there were three parameters with two levels for each parameter and orientation (Fig. 6). Interactions between
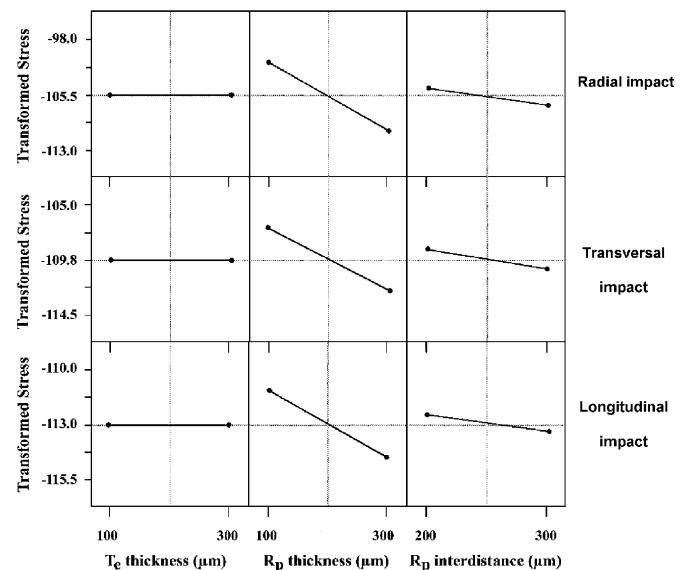

Fig. 6. Graphical representation of the interactions evaluated in the simulation. Analysis was made for the same fruit's moisture content (11%) and the same impact speed (30 m s^{-1}). Radii properties (T_e thickness, R_p thickness and R_p interdistance) were considered at two levels and three fruit's orientations (radial, transversal and longitudinal). The stress magnitudes are for the logarithmic transformation (MN_T) of the data. Simulated impact of fruits at the three orientations show the most significant interaction effect on the generated stress for the pericarp's parenchymatic rays thickness (R_p) with an effect, the difference between the two points, of approximately 5.9, 4.7 and 2.8 units respectively, being the R_p interdistance the next most significant factor with an effect of approximately 3.3, 2.2 and 0.9 units respectively. The T_e thickness factor has minimal differences in variability.

parameters were considered to determine if they influenced the results.

The two main parameters that were identified as to have affected the outcome of the FE experimental measurements were R_p thickness followed by R_p interdistance (Fig. 6). T_e

thickness did not show interaction at both levels on the magnitude of stress. The probability of these results being an artifact of statistical noise was determined by ANOVA to be less than 0.01%.

4. Conclusions

In the present study, the mechanical behavior of sunflower pericarp has been investigated by means of a computer analysis and numerical results were validated by laboratory experimental data.

The model described in this paper is a theoretical representation of the sunflower fruit's pericarp geometry, its constitutive tissues and their biomechanical properties. In any case, it is able to predict stress distribution patterns resembling the breakage pattern experimentally observed in whole fruits tested under uniaxial compression (Fig. 4A–C). It is the arrangement of the pericarp tissues, with complex biomechanical properties and different yielding strains (rays and sclerified parenchyma) which determines its response to the applied loads or under impact.

It is seen that the closest values between the fracture stress, calculated from laboratory tests in whole fruits and in the simulation where present at the site of impact. It suggest that in this place the structure will suffer an irreversible damage that will drive the complete structure to collapse.

Even though the FE model described here is a simplified version of the fruit, the results obtained can confirm the validity of the simulation. It was able to detect the effects of the impact during the hulling process. In this sense the model allows to evaluate combined effects of material properties and geometry of the sunflower fruits.

As far as we know, this is the first simulated demonstration of a sunflower pericarp breakage pattern based on the mechanical properties and the distribution of its tissues. The development of this model may be considered a starting point to define in a more accurate way, the morphological characteristics of the pericarp that determine its hulling ability, something that may be very difficult to solve with an empirical approach.

Acknowledgements

References

Baldini, M., & Vannozzi, G. P. (1996). Crop management practices and environmental effects on hullability in sunflower hybrids. *Helia, 19*, 47–62.

Beauguillaume, A., & Cadeac, F. (1992). Elements of explication of the variability of the hulling ability in sunflower. In *13th international sunflower conf. procs.* (pp. 993–999).

Boudet, A. M., Kajita, S., Grima-Pettenati, J., & Goffner, D. (2003). Lignins and lignocellulosics: A better control of synthesis for new and improved uses. *Trends in Plant Science, 8*, 576–581.

Dar, F. H., Meakin, J. R., & Aspden, R. M. (2002). Statistical methods in finite element analysis. *Journal of Biomechanics, 35*, 1155–1161.

Dedio, W. (1993). Regression model relating decortication of oilseed sunflower hybrids with achene characteristics. *Canadian Journal of Plant Science, 73*, 825–828.

Dedio, W., & Dorrell, D. G. (1998). Factors affecting the hullability and physical characteristics of sunflower achenes. *Canadian Institute of Food Science and Technology Journal, 22*, 143–146.

Denis, L., Coelho, V., & Vear, F. (1994). Pericarp structure and hullability in sunflower inbred lines and hybrids. *Agronomie, 14*, 453–461.

Denis, L., Dominguez, J., & Vear, F. (1994). Inheritance of "hullability" in sunflower (*Helianthus annuus* L.). *Plant Breeding, 113*, 27–35.

Denis, L., & Vear, F. (1996). Variation of hullability and other seed characteristics among sunflower lines and hybrids. *Euphytica, 87*, 177–187.

Dorrell, D. G., & Vick, B. A. (1997). Properties and processing of oilseed sunflower. In A. A. Schneiter (Ed.), *Sunflower technology and production* (pp. 709–745). Madison, WI: ASA, CSSA & SSSA.

Esau, K. (1977). *Anatomy of seed plants*. New York: John Wiley & Sons.

Fick, G. N., & Miller, J. F. (1997). Sunflower breeding. In A. A. Schneiter (Ed.), *Sunflower technology and production* (pp. 395–439). Madison, WI: ASA, CSSA & SSSA.

Gupta, R. K., & Das, S. K. (2000). Fracture resistance of sunflower seed and kernel to compressive loading. *Journal of Food Engineering, 46*, 1–8.

Hepworth, D. G., & Vincent, J. F. V. (1998). Modelling the mechanical properties of xylem tissue from tobacco plants (*Nicotiana tabacum* "Samsun") by considering the importance of molecular and micromechanisms. *Annals of Botany, 81*, 761–770.

Leprince-Bernard, M. N. (1990). Aptitude au Decorticage de la Graine de Tournesol. Ph.D. Thesis, Nantes Univ., France, 136 pp.

Lindström, L. I., Pellegrini, C. N., & Hernández, L. F. (2000). Anatomy and development of the pericarp in fruits of different sunflower (*Helianthus annuus* L.) genotypes. In *15th international sunflower conf. procs.* (pp. 13–18).

Logan, D. L. (2001). *A first course in the finite element method using Algor*. New York: Brooks-Cole.

Morrison, W. H., III, Akin, D. E., & Robertson, J. A. (1981). Open pollinated and hybrid sunflower seed structures that may effect processing for oil. *Journal of the American Oil Chemists Society, 58*, 969–972.

Niklas, K. J. (1992). *Plant biomechanics*. Chicago: Univ. of Chicago Press.

Pilate, G., Guiney, E., & Halpin, C. (2002). Filed pulping performances of transgenic trees with altered lignification. *Nature Biotechnology, 20*, 607–612.

Preston, R. D. (1974). *The physical biology of plant cell walls*. London: Chapman.

Ralph, J., MacKay, J. J., & Hatfiled, R. D. (1997). Abnormal lignin in a lobolly pine mutant. *Science, 277*, 235–239.

Rowe, N. P., & Speck, T. (2000). Biomechanical variation of non-self-supporting plant growth habits: A comparison of herbaceous and large-bodied woody plants. In C. Edelin (Ed.), *L'Arbre, Biologie et Developpement, Naturalia Monspeliensia. Numéro hors série* (vol. A7, pp. 1–11). .

Ruzin, S. E. (1999). *Plant microtechnique and microscopy*. Oxford: Oxford Univ. Press.

Seiler, G. J. (1997). Anatomy and morphology of sunflower. In A. A. Schneiter (Ed.), *Sunflower technology and production* (pp. 67–111). Madison, WI: ASA, CSSA & SSSA.

Thibaut, B., Gril, J., & Fournier, M. (2001). Mechanics of woods and trees: Some new highlights for an old history. *Comptes Rendus de l Academie des Sciences Serie II, 329*, 701–716.

Tranchino, L., Melle, F., & Sodini, G. (1984). Almost complete dehulling of high oil sunflower seed. *Journal of the American Oil Chemists Society, 61*, 1261–1265.

Wainwright, S. A., Biggs, W. D., Currey, J. D., & Gosline, J. M. (1982). *Mechanical design of organisms*. Princeton: Princeton Univ. Press.

Whetten, R. W., Mackay, J. J., & Sederoff, R. R. (1998). Recent advances in understanding lignin biosynthesis. *Annual Review of Plant Physiology and Plant Molecular Biology, 49*, 585–609.